

Fabrication, Characterization and Application of an Ultra Micro Ring Electrode Array

Yijin Li^{1,*}, Shanhong Xia²

¹ School of Mechanical Electronic and Information Engineering, China University of Mining & Technology-Beijing, Beijing, China

² State Key Laboratory of Transducer Technology, Aerospace Information Research Institute, Chinese Academy of Sciences, Beijing, China

*E-mail: Kathy_91@163.com

Received: 1 February 2022 / Accepted: 3 March 2022 / Published: 5 April 2022

An ultra micro ring electrode array (UMREA) was developed. The fabrication, characterization and application of the UMREA were studied. The UMREA was fabricated by standard MEMS techniques. Electrochemical measurements and SEM were used to characterize the performance of the UMREA. Owing to the small scale, the UMREA worked in typical hemispherical diffusion mode with a high mass transfer rate, which showed advantages in rapid and sensitive electrochemical measurements. Electrodeposition can also be performed on the UMREA in a short time. A comparison was made for UMREAs with different average radii. UMREA-25 was chosen by comprehensive consideration of sensitive response and modification controllability. By immobilizing microorganisms, the modified UMREA can be used in the rapid detection of BOD. Thus, the UMREA exhibits good electrochemical properties, which shows potential in sensitive measurements and sensor construction.

Keywords: Ultra micro ring electrode array (UMREA), electrochemical characterization, biochemical oxygen demand

1. INTRODUCTION

An ultramicroelectrode (UME) is a device with at least one critical dimension less than 25 μm [1]. Since its introduction into electrochemistry in the 1980s, UMEs have attracted much attention and have been applied to fields such as energy [2,3], material [4,5], the environment [6,7] and health [8,9]. One of the most important applications is fabricating sensors [10]. Due to its excellent electrochemical properties, including a high mass transfer rate, enhanced signal-to-noise ratios, decreased ohmic drop and lower double-layer capacitance [11,12], UME is especially suitable for rapid and sensitive measurements.

Many different types of UMEs have been reported, including microdisc electrodes [13], microband electrodes [14], microwire electrodes [15], micro ring electrodes [1] and needle-type

microelectrodes [16]. Among the different types, micro ring electrodes have a uniform current distribution and can easily reach stability. In addition, their current density is higher, and the response time is shorter [17]. However, these advantages of micro ring electrodes have been theoretically analyzed and numerically simulated [1,17]. The fabrication and characterization of micro ring electrodes have not been elaborately studied with experiments.

Due to the small size of UMEs, the current responses are usually on the order of magnitude of nA or pA. To overcome the limited current response one UME generates, an ultramicroelectrode array (UMEA) has been developed to magnify signals and maintain the excellent electrochemical characterizations of a single UME [18]. Many methods can be employed to fabricate UMEAs. Among them, fabrication based on MEMS techniques shows the advantages of good consistency and friendliness to system integration.

Biochemical oxygen demand (BOD) is an important index for defining organic water pollution and indicating water quality [19]. Superfluous organics in water lead to intensive metabolism of aerobic bacteria, increased consumption of dissolved oxygen, immoderate growth of anaerobic bacteria and generation of H_2S , NH_3 and CH_4 , which finally cause the deterioration of water quality [20]. By measuring the dissolved oxygen consumed during microbial metabolism, the BOD can be calculated. BOD comprehensively reflects the extent of organic pollution and water's self-cleaning capacity. Thus, rapid and accurate BOD detection is urgently needed.

The standardized method for BOD measurement is the 5-day method (BOD_5) which requires 5 days and complicated operations. Since Karube I. and Matsunaga T. [21] developed the first microbial sensor for fast BOD detection in 1977, an increasing number of studies have focused on this field. A common structure of a BOD microbial sensor consists of a microbial membrane and an oxygen permselective membrane over the electrode. The microbial membrane is used as the recognition element to metabolize organics. This process transfers the organic content to the dissolved oxygen consumption. The oxygen permselective membrane ensures the selective penetration of dissolved oxygen. Both membranes must be replaced after a period of time to avoid blockage. Another problem is that the two-layer structure increases mass transfer resistances, which is not appropriate for rapid detection. In our previous study [22], a single layer structure using electrodes as the support for microorganism immobilization was studied. With the simplified structure, the mass transfer resistance was reduced, which facilitated a fast current response. However, the integration of ultramicroelectrodes and simplified structures has not been reported.

In this paper, an ultra micro ring electrode array (UMREA) was proposed. Its fabrication, characterization and application were discussed. Standard MEMS techniques were used to fabricate the UMREA. The diffusion mode, response feature and electrodeposition performance were studied. Electrochemical measurements and SEM were used for the characterization. A comparison was made for UMREAs with different average radii. By modifying the microbial membrane through self-assembly method and covalent bonding, the application of the modified electrode to BOD detection was analyzed.

2. EXPERIMENTAL

2.1. Reagents and apparatus

AZ1500 (photoresist) was obtained from AZ Electronic Materials. Dichloroethane (EDC), N-hydroxysuccinimide (NHS), 3-mercaptopropionic acid (MPA) and gold (III) chloride trihydrate ($\text{HAuCl}_4 \cdot 3\text{H}_2\text{O}$, Au%>48%) were purchased from Sigma-Aldrich. Cells of the *Bacillus subtilis* strain (1.88) were obtained from the Institute of Microbiology, Chinese Academy of Sciences, and stored at 4 °C. Ferricyanide solution (2 mM) was prepared with 0.1 M KCl solution. Phosphate buffer solution (PBS, 5 mM) was prepared by mixing KH_2PO_4 and Na_2HPO_4 . BOD standard stock solutions (GGA) were prepared by dissolving 1.705 g glucose and 1.705 g glutamic acid in 1 L of prepared PBS at a BOD concentration of 2500 mg/l. Other concentrations of GGA were prepared by dilution before use. All other chemicals were of analytical grade and were used without further purification. Deionized water was used throughout the experiment.

Electrochemical experiments were performed with a Gamry Reference 600 electrochemical measurement system (Gamry Instruments Co., Ltd., USA). The concentration of dissolved oxygen (DO) was measured by a commercial DO meter - Eutech CyberScan DO110 Dissolved Oxygen Meter, Vernon Hills, IL, USA. SEM analysis was carried out on an S-4800 field emission scanning electron microscope produced by Hitachi (Tokyo, Japan).

2.2 Fabrication of the UMREA

The UMREA was fabricated by standard MEMS techniques. The fabrication procedures are schematically illustrated in Fig. 1. First, a Au disk electrode was fabricated on a glass wafer by photolithographic, sputtering and lift-off techniques (Fig. 1 (1-4)). Ta was needed to enhance adhesion. The thickness of the Ta layer is 300 Å and the thickness of the Au layer was 2000 Å. Then, SiN_x was deposited on the chip by PECVD for insulation (Fig. 1 (5)). The thickness of SiN_x was 1 µm. To pattern the array of the ring-shaped microelectrode, photoresist was used as a mask during etching the SiN_x insulating layer by RIE (Fig. 1 (6-7)). The residual photoresist was removed by acetone after etching (Fig. 1 (8)). The whole area of the exposed UMREA was 0.2 mm². Each ring in the array held a ring width of 10 µm. Four species of UMREA were designed and fabricated with average radii of 15 µm, 25 µm, 35 µm, and 45 µm, which were named UMREA-15, UMREA-25, UMREA-35 and UMREA-45, respectively. The ring electrode units held an interelectrode spacing of 20 times average radius. The array was distributed in a hexagonal pattern.

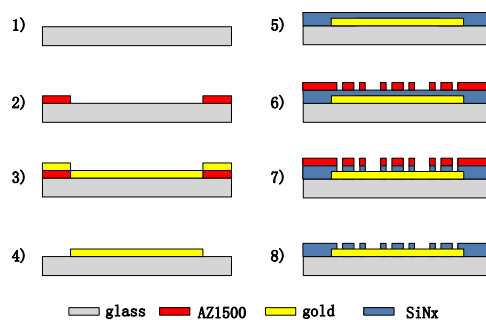


Figure 1. The fabrication procedures of the UMREA.

After the fabrication of the UMREA chip, the chip was pasted on a PCB. By pressure welding and packaging, the complete UMREA was obtained. The photo and microscope image of the fabricated UMREA are shown in Fig. 2.

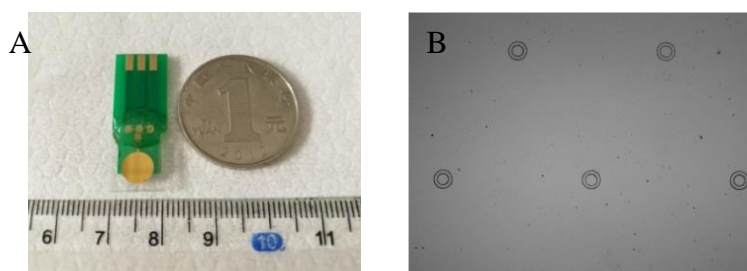


Figure 2. Photo (A) and microscope image (B) of the UMREA.

2.3 Characterization of the UMREA

Electrochemical measurements were carried out with a three-electrode cell consisting of a UMREA as the working electrode, a Pt disk ($d=1$ mm) as the counter electrode and a commercial saturated Ag/AgCl as the reference electrode. The diffusion characteristics were measured by cyclic voltammetry (CV) between -0.2 and 0.6 V in 2 mM ferricyanide solution. Different scan rates were employed from 20 to 500 mV/s.

Na_2SO_3 was used to prepare solutions with certain DO concentrations. The 0.01 M Na_2SO_3 solution corresponded to a DO concentration of 0.9 mg/L, which was detected by a Eutech CyberScan DO110 Dissolved Oxygen Meter. The response of the UMREA to DO was investigated by LSV from 0 to -1.0 V at 50 mV/s.

The feasibility of UMREA modification was tested by Au nanoparticle electrodeposition. The electrodeposition was performed by chronoamperometry at -0.3 V for 20 s in 1 mM HAuCl_4 solution. SEM and CV were used to characterize the modified UMREA. CV was performed between 0 and $+1.5$ V in 5 mM H_2SO_4 solution at 50 mV/s.

UMREA with different average radii were compared in terms of diffusion characteristics and electrodeposition performance.

2.4 Application of the UMREA in BOD detection

For application in BOD detection, the UMREA should first be modified with microorganisms. *B. subtilis* was selected for its good metabolic capacity. Its cultivation has been mentioned in ref.[22]. The harvested *B. subtilis* cells were used in the following experiments. Before electrode modification, the fabricated UMREA was electrochemically cleaned in 5 mM H₂SO₄ by CV from 0 to +1.5 V until a reduplicative curve was obtained. The UMREA was first immersed in 10 mM MPA solution for 12 h at 4 °C. The MPA-modified UMREA was washed with deionized water and dried in air. A mixture of EDC and NHS was applied to the UMREA for 15 min to activate the carboxyl groups. After activation, the UMREA was again washed with deionized water and immersed in a 6×10⁸ CFU/ml *B. subtilis* cell solution for 6 h, which ensured the bonding of the carboxyl groups on the electrode surface with the amino groups on the microorganisms. The microorganism-modified UMREA was stored in PBS at 4 °C until use. Different concentrations of GGA were detected by chronoamperometry at a potential of -0.4 V.

3. RESULTS AND DISCUSSION

3.1 Diffusion feature of the UMREA

The responses of disk electrode and UMREA with the same electrode area to 2 mM ferricyanide solution were recorded. The obtained CV curves are shown in Fig. 3. In Fig. 3A, a peak-shaped voltammogram was observed. It indicated that linear diffusion was the main diffusion mode. The diffusion process was slow. A long time was needed for reagents to move away from the electrode. With the increase of the scan rate, the redox peaks increased. The peak current was directly proportional to the square root of the scan rate, which was also a feature of linear diffusion. While in Fig. 3B, no obvious peaks were observed. The voltammogram of the UMREA was sigmoidal curve. This result was consistent with hemispherical diffusion [13]. Large steady-state limiting currents were obtained. Furthermore, when the scan rate increased, the steady-state limiting current remained the same, except for the very high scan rate of 500 mV/s. It indicated that the reagent diffusion speed was high. Thus, hemispherical diffusion is the main diffusion mode of the UMREA, which shows advantages in mass transfer and quick response.

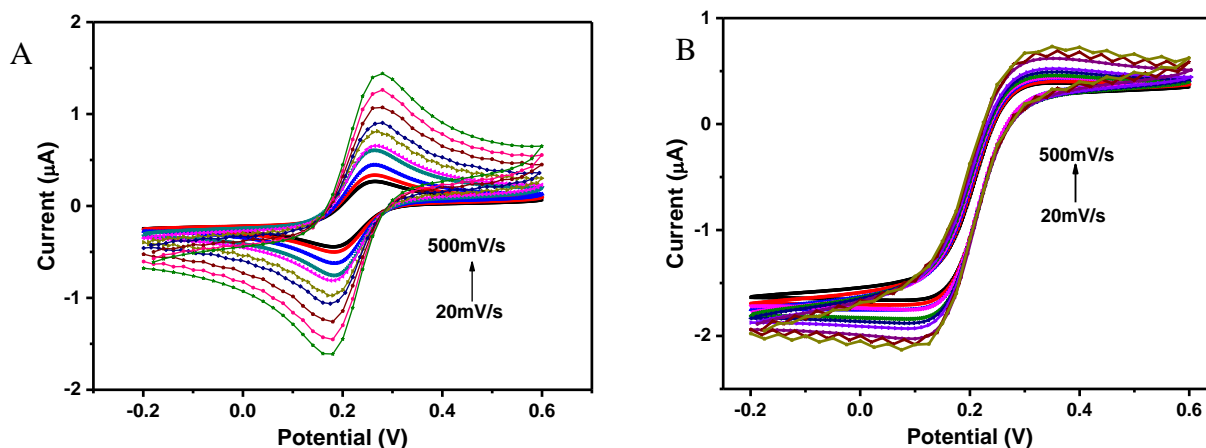


Figure 3. CV curves of the disk electrode (A) and the UMREA (B) in 2 mM ferricyanide solution with scan rates of 20, 30, 50, 75, 100, 150, 200, 300, 400, and 500 mV/s.

3.2 Response to dissolved oxygen

Dissolved oxygen was used as the analyte to characterize the response performance. PBS (5 mM, with a DO concentration of 8 mg/L measured by commercial DO meter) and 0.01 M Na_2SO_3 solution (with a DO concentration of 0.9 mg/L) were used for the contrast test. Linear scan voltammetry was utilized and the voltammograms are displayed in Fig. 4. The dissolved oxygen was reduced at approximately -0.4 V. The response of the UMREA to 0.9 mg/L DO (curve a) was lower than that of the disk electrode (curve b). The response of the UMREA to 8 mg/L DO (curve c) was much higher than that of the disk electrode (curve d). It indicated that the UMREA could effectively lower background noise and output a more effective response. The sensitivity of the measurement was obviously increased, which was in accordance with the feature of hemispherical diffusion [23]. Thus, the UMREA was more suitable for trace target measurements.

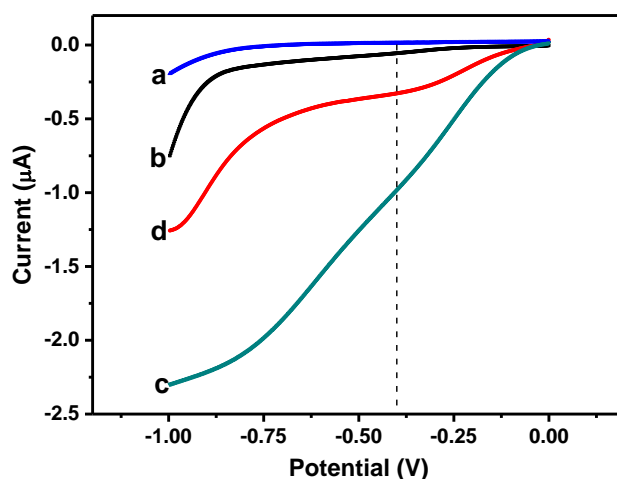


Figure 4. Linear scan voltammograms of the UMREA (a, c) and the disk electrode (b, d) in 0.01 M Na_2SO_3 solution (a, b) and PBS solution (c, d).

3.3 Electrodeposition of Au nanoparticles

Electrode modification is an important procedure to improve electrochemical performance for detection [24,25]. Thus, the performance of the UMREA after nanoparticle modification was investigated. Electrodeposition was performed at -0.3 V for 20 s in 1 mM HAuCl₄ solution. Fig. 5A shows the SEM image. Large amounts of Au nanoparticles were deposited on the surface of the UMREA. The average size of the nanoparticles was 50 nm. Due to the high current density and hemispherical diffusion mode of the UMREA, deposition could be performed in a short time.

After electrodeposition, the modified UMREA was measured in 5 mM H₂SO₄. The CV curves are shown in Fig. 5B. The oxides of gold were reduced at approximately 0.8 V, corresponding to a reduction peak. The peak current reflected the effective electrode area, which was approximately in direct proportion. As seen from Fig. 5B, the peak current before modification was -0.59 μ A at 0.83 V. After electrodeposition, the reduction potential remained the same, while the peak current increased to -1.805 μ A. This value was much larger than that of the bare electrode. Thus, the deposited Au nanoparticles can effectively increase the electrode surface.

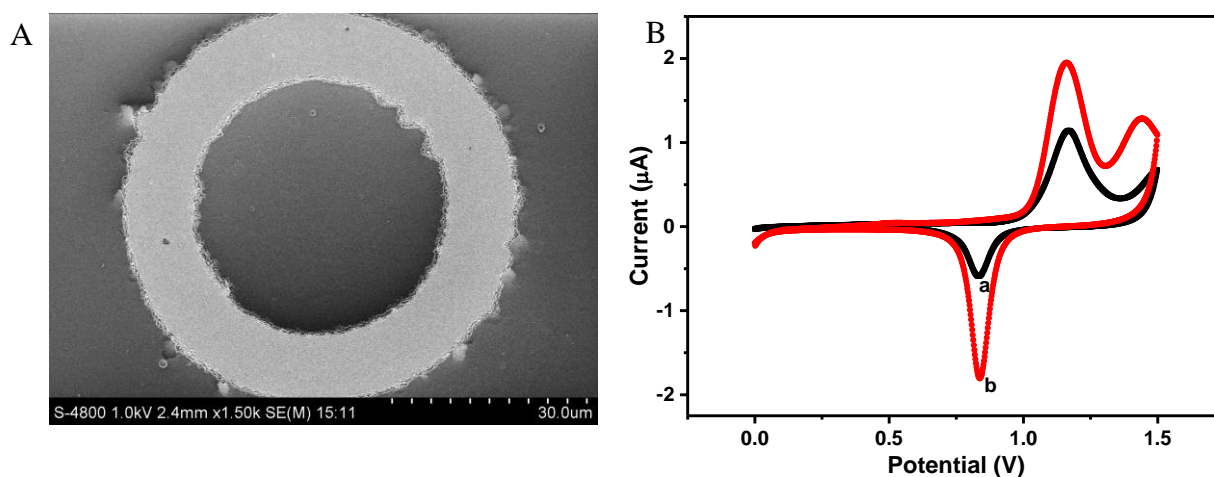


Figure 5. (A) SEM image of Au nanoparticle-modified UMREA; (B) CV curves of bare UMREA (a) and Au nanoparticle-modified UMREA (b) in 5 mM H₂SO₄.

3.4 Comparison of UMREAs with different average radii

UMREAs with different average radii have been compared in this paper. The effective working electrode area was kept 0.2 mm², and the width of the ring was kept at 10 μ m. Fig. 6 shows the CV curves obtained in 2 mM ferricyanide solution. It can be seen that the steady-state limiting current increased with the decrease of average radius. To obtain a sensitive response, a large current was preferred. Thus, UMREA-15 and UMREA-25 were further considered for the study.

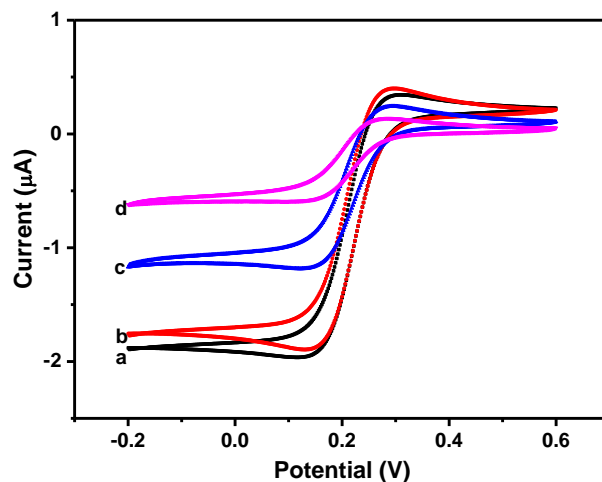
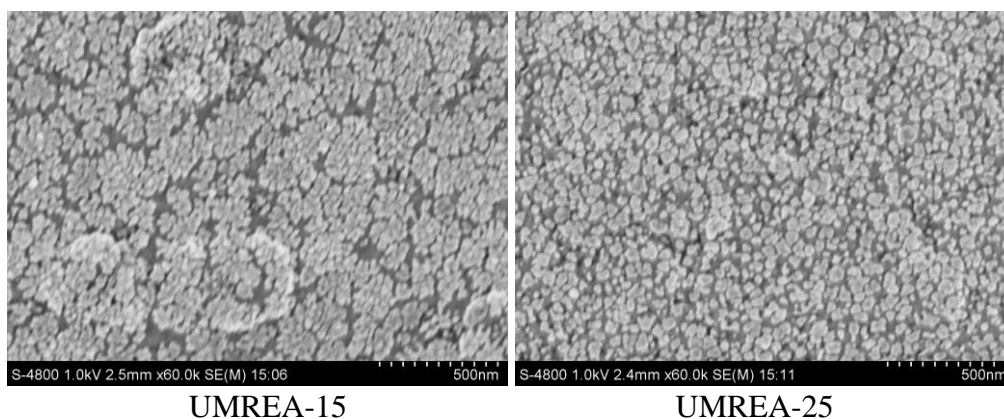


Figure 6. CV curves of UMREA-15 (a), UMREA-25 (b), UMREA-35 (c), and UMREA-45 (d) in 2 mM ferricyanide solution.

To explore the modification performance of UMREAs, electrodeposition on UMREAs with different average radii was performed at -0.3 V of 20 s in 1 mM HAuCl_4 solution. The SEM images of the modified electrode are shown in Fig. 7. The Au nanoparticles were uniformly distributed on the surfaces of UMREA-15 and UMREA-25. Due to the smaller average radius, the current density of UMREA-15 was larger, leading to more compact and overlapped Au nanoparticles. The electrodeposited Au nanoparticles on UMREA-35 and UMREA-45 were flower-spray shaped, which were not well-distributed.



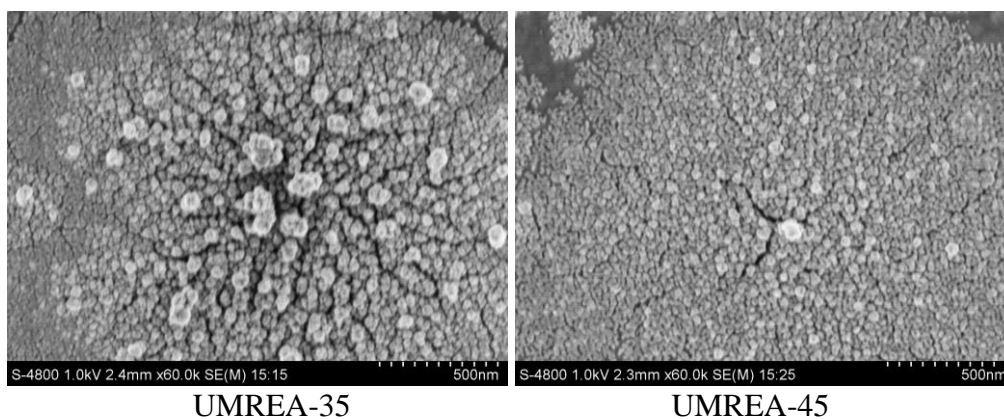


Figure 7. SEM images of Au nanoparticles electrodeposited on UMREAs with different average radii.

In summary, with the decrease of average radius, the steady-state limiting current and the current density increased. However, when the current density was too high, the controllability and consistency of electrode modification were poor. Taking both sensitive response and modification controllability into consideration, UMREA-25 was used in the following study.

3.5 Response to BOD

Fig. 8 shows the CV responses in 2 mM ferricyanide solution during the modification process. A typical sigmoidal curve was obtained on bare UMREA-25 (a). The current showed a slight decrease for MPA-modified UMREA-25 (b). It indicated that the MPA self-assembled monolayer slightly inhibited electron transfer between the electrode and redox species. Because MPA has a short carbon chain, the inhibition of electron transfer was not obvious. After bonding of amino groups of *B. subtilis* to carboxyl groups of the self-assemble layer, a further decrease in current was observed (c), owing to the immobilization of *B. subtilis* on the surface of UMREA-25.

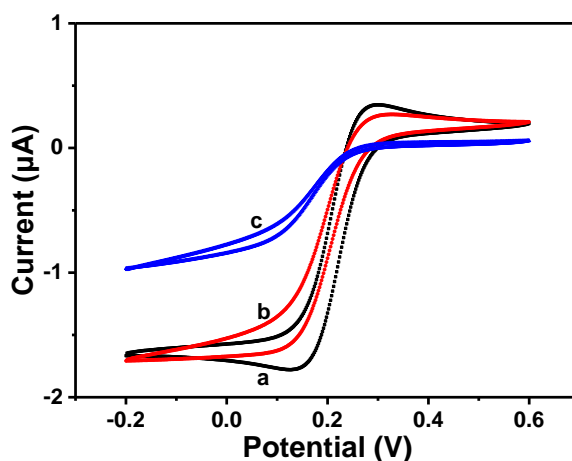


Figure 8. CV curves of bare UMREA-25 (a), MPA/UMREA-25 (b) and *B.subtilis*/MPA/UMREA-25 (c) in 2 mM ferricyanide solution.

The application of the modified UMREA-25 in detecting BOD was tested by chronoamperometry at a potential of -0.4 V. The current was registered for 5 min after UMREA-25 was immersed in PBS (background current) or GGA solution. The response to each GGA concentration was calculated as the current difference (ΔI) between the 5th minute current and the background current. The calibration curve is shown in Fig. 9. With the increasing concentration of GGA from 5 to 25 mg/L, the response current linearly increased. The linear equation is ΔI (nA) = $0.876C$ (mg/L) + 21.48, with a correlation coefficient of 0.941 and sensitivity of 0.876 nA/(mg/L). Thus, the modified UMREA-25 can be used for BOD detection. However, the sensitivity and the correlation coefficient were not good enough. Two reasons lead to this result. One is that the UMREA was not modified to specifically and sensitively respond to dissolved oxygen. The other is that the amount of immobilized microorganisms was limited. New UMREA modification method and microorganism immobilization method will be explored in a subsequent study for better application of UMREAs in BOD detection.

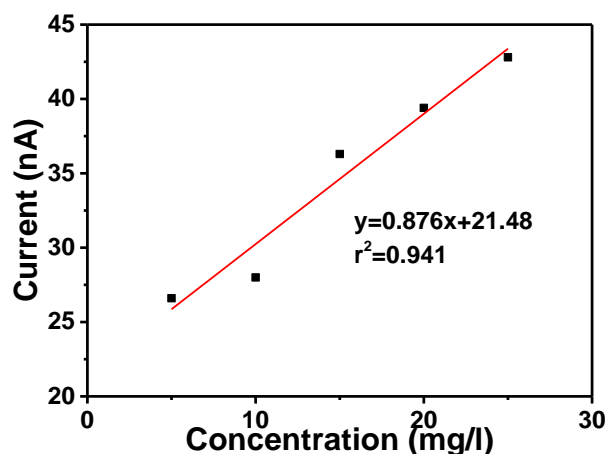


Figure 9. Calibration curve of the modified UMREA-25 to BOD.

4. CONCLUSIONS

A UME has excellent electrochemical properties due to its small scale. Although micro ring electrodes have been theoretically analyzed and numerically simulated, the characterization of UMREA with experiments has not been introduced. In this paper, the fabrication, characterization and application of an UMREA were studied. The UMREA was fabricated by standard MEMS techniques. CV and SEM were used to characterize the UMREA performance. The proposed UMREA exhibited hemispherical diffusion, leading to a high mass transfer rate, which was in accordance with the rapid electrodeposition of Au nanoparticles. The response to dissolved oxygen indicated that the UMREA was suitable for sensitive detection. UMREAs with different average radii were compared. Considering both sensitive response and modification controllability, UMREA-25 was chosen for subsequent experiments. By immobilizing microorganisms through the self-assembly method and

covalent bonding, the modified UMREA can be used in the rapid detection of BOD. Thus, the UMREA shows good electrochemical properties, which is promising for sensitive measurements and sensor construction.

ACKNOWLEDGMENTS

We acknowledge financial support from the National Natural Science Foundation of China (No. 61901476).

References

1. R. U. Rani and L. Rajendran, *Electrochem. Commun.*, 128 (2021) 107071.
2. O. Aaboubi, J. P. Chopart, A. Olivier and P. Los, *Energy Convers. Manage.*, 43 (2002) 373.
3. Q. H. Zhang, X. R. Li, P. Liu, X. Z. Meng, L. K. Wu, Z. Z. Luo and F. H. Cao, *Int. J. Hydrogen Energy*, 46 (2021) 39665.
4. L. Su, Y. Tong, T. Shu, W. Gong and X. Zhang, *Electrochem. Commun.*, 20 (2012) 163.
5. J. Delgado-Avilez, G.A. Huerta-Miranda, R. Jaimes-López and M. Miranda-Hernández, *Electrochim. Acta*, 402 (2022) 139576.
6. H. R. Lotfi Z. Z. and R. Y. Lai, *Anal. Chim. Acta*, 892 (2015) 153.
7. D. Yong, L. Liu, D. Yu and S. Dong, *Anal. Chim. Acta*, 701 (2011) 164.
8. G. Xiao, Y. Zhang, S. Xu, Y. Song, Y. Dai, X. Li, J. Xie, Y. Wang, Y. Xing and X. Cai, *Sens. Actuators, B*, 317 (2020) 128137.
9. X. Ning, Q. Xiong, T. Wu, F. Zhang and P. He, *Sens. Actuators, B*, 290 (2019) 371.
10. S. Goodwin, Z. Coldrick, S. Heeg, B. Grieve, A. Vijayaraghavan and E. W. Hill, *Carbon*, 177 (2021) 207.
11. J. Lee, Y. Seo, T. Lim, P. Bishop and I. Papautsky, *Environ. Sci. Technol.*, 41(2007) 7857.
12. U. Bruno-Mota, I. N. Rodriguez-Hernández, R. Doostkam, P. Soucy, F. Navarro-Pardo, G. Orozco, A. Yurtsever and A.C. Tavares, *Electrochim. Acta*, 402 (2022) 139524.
13. S. A. B. Shafiee, A. L. Hector and G. Denuault, *Electrochim. Acta*, 293 (2019) 184.
14. W. Zhang, Y. Xu, H. E. Tahir and X. Zou, *Chem. Eng. J.*, 309 (2017) 305.
15. S. Eloul, E. Kätelhön, C. Batchelor-McAuley, K. Tschulik and R. G. Compton, *J. Electroanal. Chem.*, 755 (2015) 136.
16. J. H. Lee, T. S. Lim, Y. Seo, P. L. Bishop and I. Papautsky, *Sens. Actuators B*, 128 (2007) 179.
17. B. Jin, W. Qian, Z. Zhang and H. Shi, *J. Electroanal. Chem.*, 417(1996) 45.
18. J. Wang, C. Bian, J. Tong, J. Sun, W. Hong and S. Xia, *Electrochim. Acta*, 145 (2014) 64.
19. S. Jouanneau, L. Recoules, M. J. Durand, A. Boukabache, V. Picot, Y. Primault, A. Lakel, M. Sengelin, B. Barillon and G. Thouand, *Water Res.*, 49 (2014) 62.
20. Y. Li, J. Sun, J. Wang, C. Bian, J. Tong, Y. Li and S. Xia, *Biochem. Eng. J.*, 123 (2017) 86.
21. I. Karube and T. Matsunaga, *Biotechnol. Bioeng.*, 19 (1977) 1535.
22. Y. Li, J. Sun, J. Wang, C. Bian, J. Tong, Y. Li and S. Xia, *Biochem. Eng. J.*, 112 (2016) 219.
23. M. Miyata, Y. Kitazumi, O. Shirai, K. Kataoka and K. Kano, *J. Electroanal. Chem.*, 860 (2020) 113895.
24. X. Chen, J. Chen, H. Dong, Q. Yu, S. Zhang and H. Chen, *J. Electroanal. Chem.*, 848 (2019) 113244.
25. Y. Li, J. Sun, J. Wang and S. Xia, *Int. J. Electrochem. Sci.*, 13 (2018) 11454.